RSC Advances

PAPER

View Article Online
View Journal | View Issue

Cite this: *RSC Adv.*, 2025, **15**, 34039

Study on the structure and properties of inclusion complexes of large ring cyclodextrin and aromatic compounds

Chuan Cao, Pingping Huang, Jing Guo and Deming Li*

Received 8th May 2025
Accepted 25th August 2025

DOI: 10.1039/d5ra03235k

rsc.li/rsc-advances

We successfully used co-precipitation to integrate four common aromatic compounds with different functional groups into macrocyclic dextrin, and we provided a detailed description of the inclusion complexes that occurred. Combining X-ray diffraction (XRD), Fourier transform infrared spectroscopy (FTIR), and nuclear magnetic resonance hydrogen spectroscopy (^{1}H NMR) allowed for confirmation of the inclusion complexes' formation. The thermal stability of the aromatic compounds is also supported by the inclusion complexes' higher structural stability. In the industrial and culinary sectors, LRCD is anticipated to function effectively as a solid matrix carrier for encapsulating aromatic chemicals.

1. Introduction

As some of the most popular biopolymers in food, pharmaceutical, and medical applications, cyclodextrins outperform other polymers in terms of biocompatibility, bioactivity, homogeneity, and bioadhesion. They have also been found to have excellent rheological and biomucoadhesive properties, which facilitate the design and development of a wide range of practical and economical sustained-release and drug delivery systems.[1] Large ring cyclodextrin (LRCD) has a hydrophobic channel-like big cavity shape, is readily soluble in water, can form inclusion complexes with a variety of guest molecules, and has a wide range of potential uses in the food science, biotechnology, and pharmacy domains. In biotechnology, LRCD has been applied as a coating to enhance paper.[2] Chemically modified LRCD (CD_9) has been shown to have a higher chemiluminescence efficiency when combined with a fluorescein analogue.[3] Furthermore, some unstable or insoluble pharmacological compounds can be dissolved and stabilised by LRCD. The development of inclusion complexes between CD_9 and several guest molecules was investigated by Ueda and his group. They discovered that CD_9 was superior to α-CD in solubilization and could further increase the solubility of digoxigenin and spironolactone.[4] Meanwhile, CD_9 can form an inclusion complex with C_{60},[5] and its solubility in water is better than that of γ-CD.[6] Rutin and thymoquinone are delivered concurrently to aid in wound healing using cyclodextrin and a PVP-stable nanocrystalline gel.[7] Additionally, other studies have examined LRCD with varying levels of polymerisation embedded in nystatin, ibuprofen, flurbiprofen, and butyl benzoic acid, which improved the drug's stability and utilisation rate. In order to reduce the entropy of the system,[8] LRCD, which has a degree of polymerisation ranging from 22 to 100, combines with iodide and other substances to form a complex. The degree of polymerisation of LRCD, the structure of host–guest molecules, the hydrogen bonds and van der Waals forces of host and guest molecules, and the size of intermolecules have all been linked to the complex development of LRCD, according to a number of studies.[9] Using cyclodextrin glucosyltransferase (CGTase), Cao synthesised macrocyclodextrins (LR-CDs, CD9–CD22) from rice starch and used them as embedding agents for α-tocopherol and *Litsea cubeba* essential oil. Enhancing α-tocopherol's thermal stability using microencapsulation can regulate the essential oils' delayed release and extend the antibacterial activity's duration. An excellent wall material for embedding essential oils is LRCD.[10,11] The present findings offer an experimental foundation for the use of LRCD in food preservation and the delivery of functional active ingredients. However, they also highlight the need for additional research, as the majority of previous studies have concentrated on the inclusion effect of a single kind of guest molecule (like phenols and essential oil mixtures) with LRCD, leaving the precise interaction and inclusion mechanism between aromatic compounds with various functional groups and LRCD unclear.

A class of chemical molecules with unique scents, antibacterial qualities, and antioxidant capabilities were known as aroma compounds. Citral and delta-decalactone smelt like lemon and peach, and carvone had strong antibacterial properties against both germs and fungi. Furthermore, the food and chemical industries made extensive use of aroma compounds for a variety of purposes, including baking, candies, drinks, active packaging, fruit and vegetable preservation, and as components of food flavourings and cosmetic perfumes.[12] During processing and storage, embedding is the best method to minimise evaporative losses and lower their volatility. The

Anhui University of Applied Technology, Hefei 230011, China. E-mail: ldm@uta.edu.cn; 877542357@qq.com

complexes that are created when LRCD and aromatic chemicals interact can reduce the volatility of aroma compounds and produce a steady release of hydrophobic active ingredients that are tiny molecules.

The aroma compounds chose four C10 aromatic molecules with different structures (acid, lactone, ketone, and aldehyde) as the core material, and LRCD was chosen as the wall material. These molecules are open-chain monoterpenes (citral, Cit), cycloalkyl molecules (carvone, Car), lactone molecules (δ-decanolide, Dec), and straight-chain alkyl molecules (*n*-decanoic acid, Decd). With the inclusion of essential oils and tocopherol as the foundation for earlier research, this study provides a new scientific basis for food flavor preservation and stable delivery of functional fragrances by revealing for the first time at the molecular level the specific interaction law between LRCD and aromatic compound functional groups. The acquired data can be used to investigate the atomic stability of LRCD and to gain an intuitive understanding of the interactions between LRCD and guest molecules.

2. Experiment

2.1. Materials

Aladdin Reagent Co., Ltd supplied citral, carvone, decanoic acid, and δ-decanolactone; LRCD (CD9–22) was made in the lab by combining CGTase and pullulanase from rice starch; the published article has full manufacturing instructions,[10] the degree of polymerisation of the lab-produced LRCD in our work is 9–22 because the degree of polymerisation of LRCD mixes manufactured from glutinous rice starch is primarily concentrated in the CD9–CD22 range.Sinopharm Chemical Reagent Co., Ltd supplied the other chemicals.

2.2. Preparation of LRCD

Add 5% w/v glutinous rice starch and acetic acid buffer (0.01 M, pH 5.5) to a 500 mL conical flask. After 30 minutes of boiling and stirring, the mixture should cool to 55 °C, add 100 U g^{-1} of pullulase, and incubate for 12 hours at 55 °C and pH 5.5. After 10 minutes of boiling, the mixture should cool to 60 °C, add 8 U g^{-1} of CGTase, and then incubate for an additional two hours at 60 °C and pH 5.5 to produce LRCD. Fill the bottle with 250 mL of ethanol, lets it sit at room temperature for 12 hours, and then centrifuge it for 10 minutes at 5000 rpm. The dried LRCD is obtained by collecting the pellet, washing it with anhydrous ethanol, and then vacuum-drying it at 40 °C.

2.3. Sample preparation

The mixture was prepared using the previously described procedure, with some adjustments.[13] LRCD solution chilled to 25 °C is mixed with a mixture of aroma compounds and absolute ethanol (1 : 2 v/v), and the aroma compounds are mixed with the LRCD at a molar ratio of 1 : 2. Then, vortex the mixture for five minutes. After being stored at 4 °C for 12 hours, the complex was obtained by centrifuging it for 15 minutes at 5000 r min^{-1}, collecting the precipitate, The inclusion complex is obtained by freeze-drying the precipitate after it has been cleaned with anhydrous ethanol. For later usage, keep the clathate in a drier set at 25 °C.

In order to prepare the physical mixture, the LRCD is initially ground in a mortar according to the ratio used to create the inclusion complex. After that, aromatic compounds are added to the prepared LRCD, and with scraping, the physical mixture is evenly mixed.

2.4. Measurement of encapsulation efficiency

By measuring the aroma compounds at various wavelengths using a UV-Vis spectrophotometer[14] and computing the complex's aromatic compound concentration using the methodology described in the literature,[15] encapsulation efficiency (EE) was ascertained(δ-decanolactone 206 nm, Citral 238 nm, carvone 245 nm,After the reaction of decanoic acid with bromocresol green-ethanol solution to form a colored complex, the wavelength is 620 nm). The standard curve regression equation for ethanol solutions of various aroma compounds was plotted after the aromatic compound/LRCD complex was dissolved in 95% ethanol for 24 hours and the supernatant was collected by centrifugation at 5000 r min^{-1} for 15 minutes.

The EE is calculated according to the following formula:

$$\mathrm{EE} = \frac{\text{Content of intercepted active compounds}}{\text{Initial content of active compounds}} \times 100 \quad (1)$$

2.5. Analysis of complexes

2.5.1. FT-IR. FT-IR spectroscopic analysis was carried out using the sample and potassium bromide pellet (1 : 100, w/w).[16] In an agate mortar, combine the complex powder with dried potassium bromide crystals, ground them completely, and then press them into thin sheets to create a liquid aromatic powder. Aroma compounds are dropped in the middle of potassium bromide crystals.

2.5.2. XRD. According to previous method,[17,18] X-ray diffractometry was used to determine the sample's crystal structure. The scanning area was 0–50°, and the scanning rate was 2° min^{-1}. MDI Jade 6.0 software was used to record the samples' crystal type and crystallinity.

2.5.3. ^{1}H NMR spectra. Using the earlier technique, an NMR spectrometer measured the samples' ^{1}H NMR spectra.[14] D_2O (0.5 mL) is used to dissolve the sample. In ppm, chemical shift (δ) is expressed. Calculated Chemical Displacement Difference ($\Delta\delta$) based on the following formula: $\Delta\delta = \delta(\text{complex}) - \delta(\text{free})$.

δ(free) is LRCD, δ(complex) is the chemical displacement of the clathrate's hydrogen protons, and $\Delta\delta$ is the chemical displacement difference.

The hydrogen proton's chemical shift.

2.5.4. Thermodynamic analysis. With a nitrogen flow of 50 mL min^{-1}, the samples' thermodynamic characteristics were examined using a Netzsch integrated thermal analyser at a rate of 15°C min^{-1} from 50 °C to 600 °C.[19]

2.6. Statistical analysis of data

Three parallels were used for all of the aforementioned studies, and the mean ± standard deviation was used to express the results. For the study of significant differences ($P < 0.05$), SPSS statistical software version 21.0 was utilised.

3. Results and discussion

3.1. Examine the effects on encapsulation of aromatic chemicals embedded in LRCD

Fig. 1 illustrates the encapsulation effectiveness of the complexation of several aroma compounds with LRCD. Through enzymatic modification, starch is transformed into CD molecules with stable physicochemical characteristics that can combine with a range of organic substances to form complexes. Complexing organic molecules with CD can change their solubility, make them more stable in the presence of heat, light, and oxidation, and decrease their volatility.[20] Due to its special cavity structure, cyclodextrin can form inclusion complexes by encasing guest molecules inside it. The figure shows that the embedding efficiency varies between 39.18% and 78.99%, with carvone having the highest embedding rate and δ-decanolactone having the lowest. The primary causes of the variation in embedding efficiency are as follows: functional groups have varying affinities for CD, and molecules in solution either form inclusion complexes or retain them in solution in varying amounts depending on their equilibrium point.[21] The substance and LRCD interact differently, and the guest molecule's physicochemical characteristics and chemical structure alter.[22] The physical mixture's low encapsulation that we saw could be the result of the sample's guest molecules' adsorption mistakes.

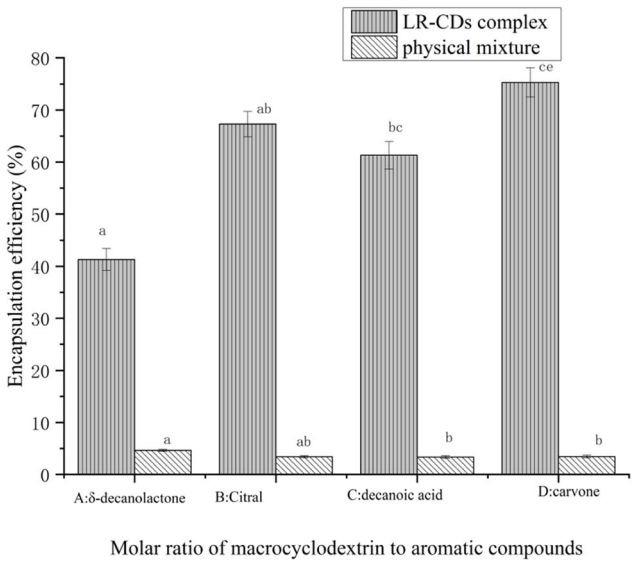

Fig. 1 Encapsulation efficiency of different aromatic molecules complexed with LRCD (there were substantial differences in small letters ($p < 0.05$)).

3.2. FT-IR analysis

The FTIR spectra of the LRCDs, physical mixes, inclusion complexes, and aroma compounds are shown in Fig. 2. C═O stretching vibrations are represented by the characteristic peaks of δ-decanolactone and carvone at 1777 and 1671 cm^{-1}, C–O–C stretching vibrations by the peak at 1181 cm^{-1}, and ketone groups connected with C–C stretching vibrations by the peak at 1100 cm^{-1}. The stretching vibrations of the methyl and methylene groups[23] are linked to the peaks between 1200 and 1400 cm^{-1}, whilst the CH stretching vibrations of the methyl group are represented by the peaks between 2858 and 2930 cm^{-1}. Unlike LRCD, the spectra of their inclusion complexes hardly show the distinctive peaks of δ-decanolactone (1777 cm^{-1}) and carvone (1671 cm^{-1}), suggesting that the guest molecule and wall material are complexed. The formation of the inclusion complex is confirmed by the newly detected peaks in the embedding at 1636 cm^{-1} and 1633 cm^{-1}, which show the formation of hydrogen bonds between the hydroxyl group of the LRCD and the carbonyl group of esters and ketones.

The stretching vibration of CH is indicated by the two separate bands of citral at 2820 and 2720 cm^{-1}, whereas the stretching vibration band of C═O was visible at 1670 cm^{-1}. Decanoic acid's FTIR spectra show characteristic bands at around 937, 1713, and 2925 cm^{-1}. The C═O and OH vibrations in carboxylic acids are represented by the peaks at 1713 and 937 cm^{-1}, respectively, whereas the CH–H stretching vibration bands from $–CH_2–$ and $–CH_3$ are observed at 2855 and 2925 cm^{-1}, respectively.[24] The inclusion complex's spectrum was quite similar to that of capric acid, but the carbonyl peak is much reduced, and a new peak appears at 1024 cm^{-1}, indicating that most of the capric acid was complexed. The formation of successful inclusion complexes between LRCD and the capric molecule is further indicated by the shift of carbonyl resonance to higher wavenumbers (937 to 1024 cm^{-1}). The disruption of hydrogen bonds between the carboxyl groups in the capric acid molecule and the formation of hydrogen bonds between the carbonyl and hydroxyl groups of dextrin are responsible for the change in the carbonyl resonance region. This allows the guest molecule to be encapsulated within the cavity structure of dextrin.[25]

Previous reports indicate that the incorporation of guest molecules diminishes both the motility and signal intensity of the encapsulated molecules.[26,27] The alterations observed in the characteristic bands of the guest molecule, including reductions, disappearances, and the broadening of peak intensity, can be ascribed to the constraints imposed on the tensile vibrations of the guest molecule within the confines of the CD cavity. This phenomenon suggests the formation of an inclusion complex between the guest molecule and the wall material.[15]. Furthermore, the absorption bands corresponding to the O–H bend (3308 cm^{-1}), OH bend (1641 cm^{-1}), and C–O–C bend (1030 cm^{-1}) of the glycosidic bond exhibited minimal variation when compared to LRCD. The findings indicated that the characteristic peaks of LRCD and aroma compounds were present within this complex. The reduction in the peak signal of the two components suggests a molecular interaction; however,

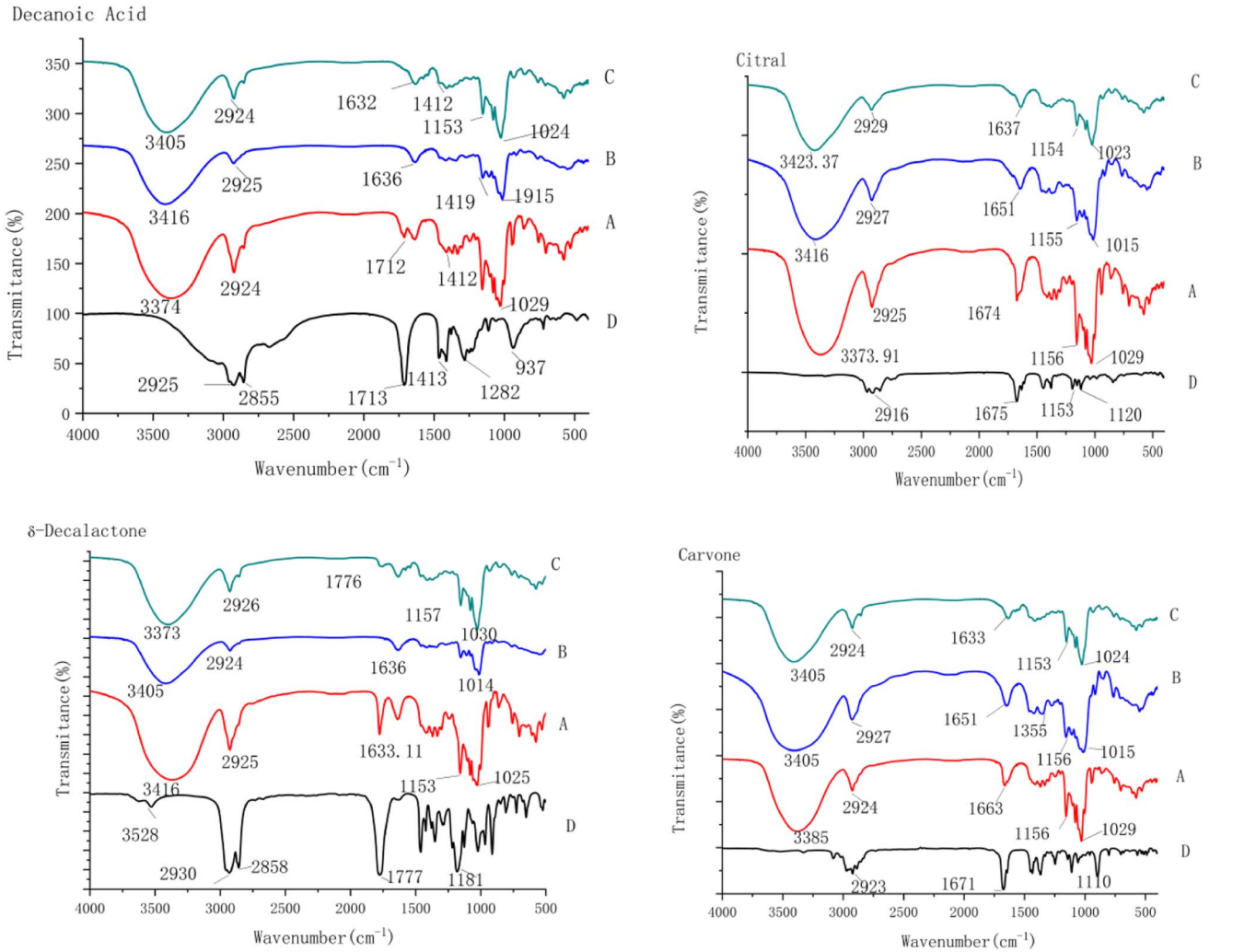

Fig. 2 FTIR spectra of LRCD (A), physical mixture (B), inclusion complex (C) and free aroma compounds (D).

the vibrational frequency band remains unchanged. This phenomenon contrasts with the embedding observed between small CDs and guest molecules, where alterations in the signature peaks of guest molecules are generally mentioned.[28]

The physical mixture's distinctive absorption bands reveal the overlaid combination of the LRCD's and the aromatic compound's unique spectrum characteristic peaks, suggesting minimal molecular interaction. The stretching of C=O, O–H, and C–H, respectively, was assumed to be the cause of the distinctive bands seen in the FT-IR spectra of aroma compounds at 1750, 955, and 2928 cm^{-1}.[29] The stretching of O–H and C–O–C is assumed to be the cause of the distinctive bands seen in the LRCD's FTIR spectra at 3308 and 1030 cm^{-1}, respectively. Furthermore, the characteristic peak related to OH was extended and changed from 3321 to 3308 cm^{-1} when the inclusion complex was compared to LRCD. This suggests that there was a notable increase in the hydrogen bonding between LRCD and aromatic molecules.

3.3. Crystal structure of aromatic compound inclusion compounds with embedded LRCD

Each ordered structure formed by aroma compounds/LRCD complexes has a distinct X-ray diffraction pattern and varying degrees of crystallinity (Fig. 3). The structural formulae of the chosen aroma compounds are listed in Table 1. We chose aroma compounds with distinct functional groups to form complexes with LRCD for investigation because of the significant similarities in crystal structure and thermal characteristics between complexes generated with other aroma compounds. With δ-decanolactone complexes, the LRCD displays distinctive peaks at 6.9°, 10.8°, and 17.2°. There are two spikes (about 10.8°, 17.2°) and two neighbouring peaks (around 13.8, 14.2). The most probable explanation is that the guest molecule embeds itself in the helical centre cavity due to the intermolecular van der Waals force interaction and hydrogen bonds between the hydrocarbon chain and the internal helical cavity.[24]

The complex guest molecular structure is stabilised by the van der Waals forces molecules interaction between the inner spiral cavity and the short C6-based aliphatic short chain in δ-

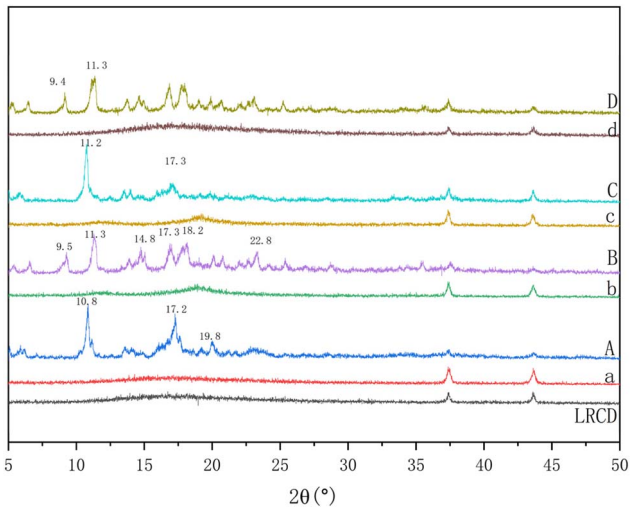

Fig. 3 X-ray diffractograms of the inclusion compound of LRCD with different aroma compounds. (abcd stands for physical mixture, ABCD stands for inclusion complex, where A is δ-decanolactone inclusion, B is Citral inclusion, C is decanoic acid inclusion, D is carvone inclusion).

decolide. The lactone ring occupies a large helical space, and there is more space between the helices. The lactone guest may be partially contained in the cavity and appear between the helices, forming the corresponding structure. The LRCD's large primary peak of the δ-lactone complex and comparatively low crystallinity may be explained by this. In contrast, samples containing complexes of LRCD and capric acid showed comparable peaks at 6.8°, 11.2°, and 17.3°. Because they are linear ligands with a lower cross-section and occupy less space, decanoic acid molecules (also known as linear alkyl chains) are only found in the helical cavity, which promotes a densely packed crystal structure between the helix and the linear ligand.[30]

Table 1 Structural characteristics of aroma compounds

Aroma compounds	Structural formula	Molecular formula
δ-Decalactone	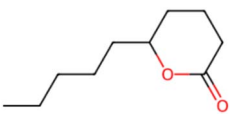	$C_{10}H_{18}O_2$
Citral	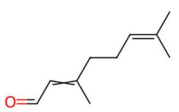	$C_{10}H_{16}O$
Decanoic acid	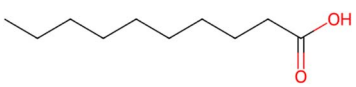	$C_{10}H_{20}O_2$
Carvone	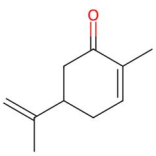	$C_{10}H_{14}O$

The LRCD complexes with citral and carvone showed distinct diffraction peaks. According to Nimz's research, alcohols and acids can both donate and accept hydrogen bonds, whereas aldehydes can only accept them. This means that both alcohols and acids' oxygen atoms can form hydrogen bonds at the helical inlet, but citral has fewer interactions with aldehyde groups, which results in comparatively weak stability and crystallinity.[31] Carvone complexes have been observed to exhibit diffraction patterns similar to those of alcohols and aldehydes, despite the fact that the six-membered litones in carvone are larger than those of menorolide. It's possible that the guest molecule's functional group structure interacts with the LRCD molecule, and that the primary forces for the creation of clathrates in the solid state are van der Waals forces, hydrogen bonds, and electrostatic forces.[32]

3.4. ^{1}H NMR analysis

We examined the structural characteristics of the inclusion complex made up of LRCDs and aromatic molecules using hydrogen nuclear magnetic resonance (^{1}H NMR) spectroscopy; Fig. 4 displays the correlation spectra. This technique is well known for its capacity to identify minute alterations in the proton chemical environment brought on by host–guest interactions and is a reliable way to confirm that inclusion complexes[29] are formed. We discovered a number of spectrum characteristics that were crucial to the inclusion complex's successful development when we compared the ^{1}H NMR spectra of pure LRCD, free aromatic compounds (citronellaldehyde, carvone, δ-decanolactone, and *n*-capric acid), and their corresponding inclusions: first, inconsistencies in the proton chemical shift of LRCD were revealed by the inclusion spectra. In particular, the LRCD lumen's protons ($\Delta\delta$ = 0.05–0.12 ppm) were considerably displaced in comparison to pure LRCDs.[33] When guest molecules enter the LRCD cavity, their hydrophobic aromatic groups act as a shield, interacting with both the guest molecule's electron density and the surface electron π density of the inner cavity, which is rich in C–H bonds. This is the cause of this displacement. Second, additional evidence is provided by variations in the proton signal of aromatic compounds. In the free state, for instance, the aldehyde-based protons of citral show a low field displacement of roughly 0.10 ppm ($\delta \approx 5.77$ ppm). In the LRCD cavity, the citral-aldehyde group that is partially exposed to polar water in the free state experiences a higher shielding effect. Changes in the electronic environment of guest molecules during inclusion are reflected in these shifts. Furthermore, compared to free aromatic compounds normalized based on a proton signal of roughly 3.28 ppm in the LRCD, the peak intensity of guest molecules in the complex spectrum varies significantly. This suggests that the guest molecules move during inclusion, which is consistent with their confined state within the LRCD cavity. The creation of the inclusion complex was strongly confirmed by the combined study of spectrum features: the retention of the LRCD backbone signal, the decrease in guest proton intensity and the change in

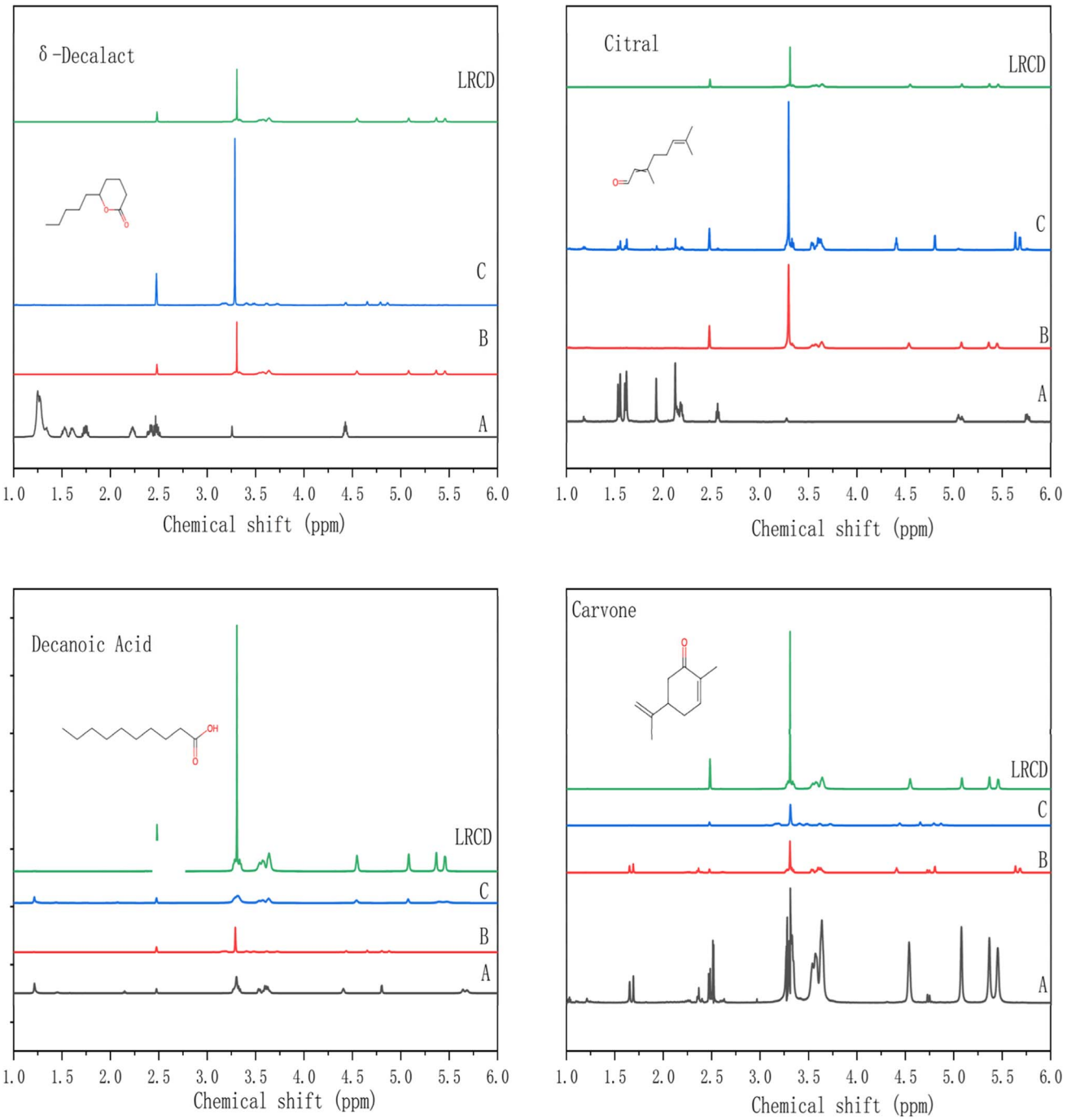

Fig. 4 ^{1}HNMR chart of the inclusion compound of LRCD and different aromatic compounds. A: aromatic compound B: physical mixture C: inclusion compound.

chemical displacement, and the proton displacement of the cavity in the LRCD. When coupled with the complimentary findings of FTIR.

3.5. Thermodynamic analysis

3.5.1. Thermo gravimetric analysis (TGA). The TG curves of the physical mixture and the inclusion complex are displayed in (Fig. 5), illustrating the variations in thermal stability brought about by the polarity, size, and binding force of the molecule between the LRCD and the guest for several guest molecules. The complex's thermal stability is increased by the interaction with LRCD. Decanoic acid and its complexes with straight-chain alkyl molecules exhibit better thermodynamic stability and higher cleavage temperatures. This could be because the longer alkyl chains interact more strongly with the inside of the helix due to their higher hydrophobicity, which increases their ability to reside in the hydrophobic cavity and necessitates more heat to break the hydrophobic interactions. Additionally, the

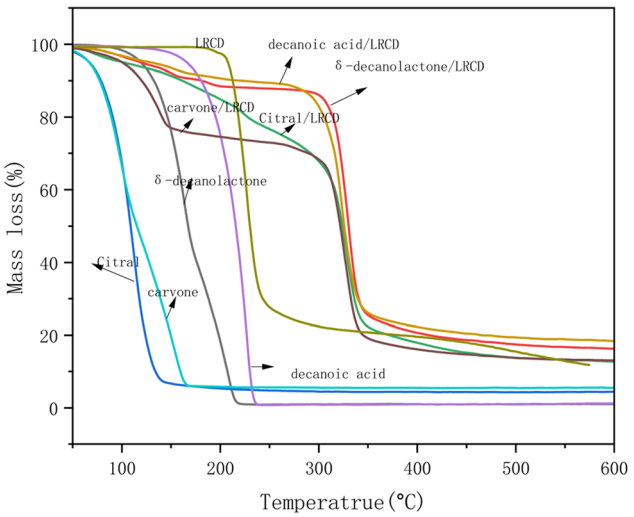

Fig. 5 TGAof different aromatic molecules complexed with LRCD.

decanoic acid has a higher cleavage temperature because it has more binding sites thanks to the carboxyl group and more hydrogen bond formation. Tight packing between helices and the creation of dense crystal structures are made possible by linear ligands with smaller cross-sections since they take up less space and are exclusively found in the helical cavity.[30] The lactone ring of δ-decanolactone may be sterically prevented from accessing the deeper helical cavity when entering a single helix, in contrast to acids, thus lactone inclusion complexes (δ-decanolactones) are lower than linear alkyl chain molecular inclusion complexes.[34] Lactones can be found both inside and between the helices due to the larger "head" of the lactone ring and the smaller "tail" of the alkyl chain, which prevents the helices from being firmly stacked.[35] A wider hole is needed to accommodate the identical six-membered naphthenic group found in carvone. Because of the helix's open configuration, there will be less chance of future nucleation, which will restrict thermal stability and crystallisation. Since citral contains many double bonds and these bonds can break when heated, the figure shows that free citral has the lowest thermal stability. Because cyclodextrin is thermally stable and some residues are remained at high temperatures, the embedding material can be seen above 600 °C with only 15% to 20% remaining. The essential oil is shielded by the embedding structure, which also delays its breakdown; inorganic salts, metal ions, and other contaminants with high thermal stability are present in the sample; there are measurement errors in thermogravimetric analysis related to heating rate control, sample consistency, and instrument precision.

The aroma compounds' TG curves demonstrate that gasification begins at 120 °C and vaporisation proceeds at a fairly rapid rate. The compounds are fully vaporised at a temperature of about 220 °C. Over 90% of weight loss happens between 150 °C and 250 °C due to the evaporation effect. The inclusion complex has strong thermal stability, and encapsulation treatment can greatly increase the thermal stability of aromatic compounds. The inclusion complex exhibits three stages of

Table 2 TGA of different aromatic molecules

	Lose weight (%)		
Sample	50–100 °C	100–200 °C	200–600 °C
A:δ-decalactone	2.8 ^{ab}	79.4^{a}	16.9^{a}
B:Citral	33.5^{c}	61.2^{b}	0.9^{b}
C:Decanoic acid	1.7^{a}	33.8^{c}	63.4^{c}
D:Carvone	34.2^{c}	60.1^{b}	1.1^{b}

Table 3 TGA of different aromatic molecules complexed with LRCD[a]

	Lose weight (%)		
Inclusions complex	50–150 °C	150–300 °C	300–600 °C
a:δ-decalactone/LRCD	9.1^{b}	15.0^{b}	69.7^{b}
b:Citral/LRCD	9.8^{b}	22.6^{a}	54.9^{c}
c:Decanoic Acid/LRCD	6.6^{c}	10.8^{c}	64.3^{b}
d:Carvone/LRCD	33.1^{a}	1.2^{d}	55.7^{c}
LRCD	0.9^{d}	13.1^{b}	73.2^{a}

[a] Note: the statistical analysis was conducted using SPSS 21.0 software, with a significance threshold of $P < 0.05$. Following the same column of data, different lowercase letters indicate significant changes ($P < 0.05$), whereas the same lowercase letters indicate no significant differences ($P > 0.05$).

decomposition, as the image illustrates. In the first stage, the mass loss from carvone reached almost 33%, while the mass loss from LRCD-related surface water was around 10%. The initial weight loss took place between 50 and 150 °C. The mass loss in the second stage, which is associated with the evaporation of the internal water and occurs at around 200 °C, is between 10 and 20%. The mass loss of carvone is also lower during this stage. The third stage, which may be connected to the LRCD degradation, takes place at about 300 °C and involves a mass loss of 50–70%.[36] Tables 2 and 3 present the specific mass loss. Furthermore, LRCD-aromatic complexes show lower overall weight loss and slower weight loss rates than free aroma compounds, indicating that molecules have more chances to entanglement and aggregation at higher temperatures.[37] We can conclude that the inclusion complex improves thermal stability and suggests that the inclusion complex is forming.

3.5.2. Differential scanning calorimetry(DSC). The DSC curve showed an absorption peak between 50 and 100 °C, which could be associated with the boiling of the guest species. The transition temperature dropped a little after the inclusion complex formed, and the action of cyclodextrin (CD) weakened the intermolecular forces of the flavour compounds, which decreased the boiling of the inclusion complex and widened the loss peak. In addition, it is possible to destroy the crystalline state of the substance and turn to an amorphous state, and the crystallinity of the compound decreases. Fig. 6 displays DSC graphs of the complexation of various aroma compounds with LRCD. There are two stages to the heating process for the full DSC analysis of the inclusion complex. The first is that as the temperature rises from 50 °C to 200 °C, the endothermic peak

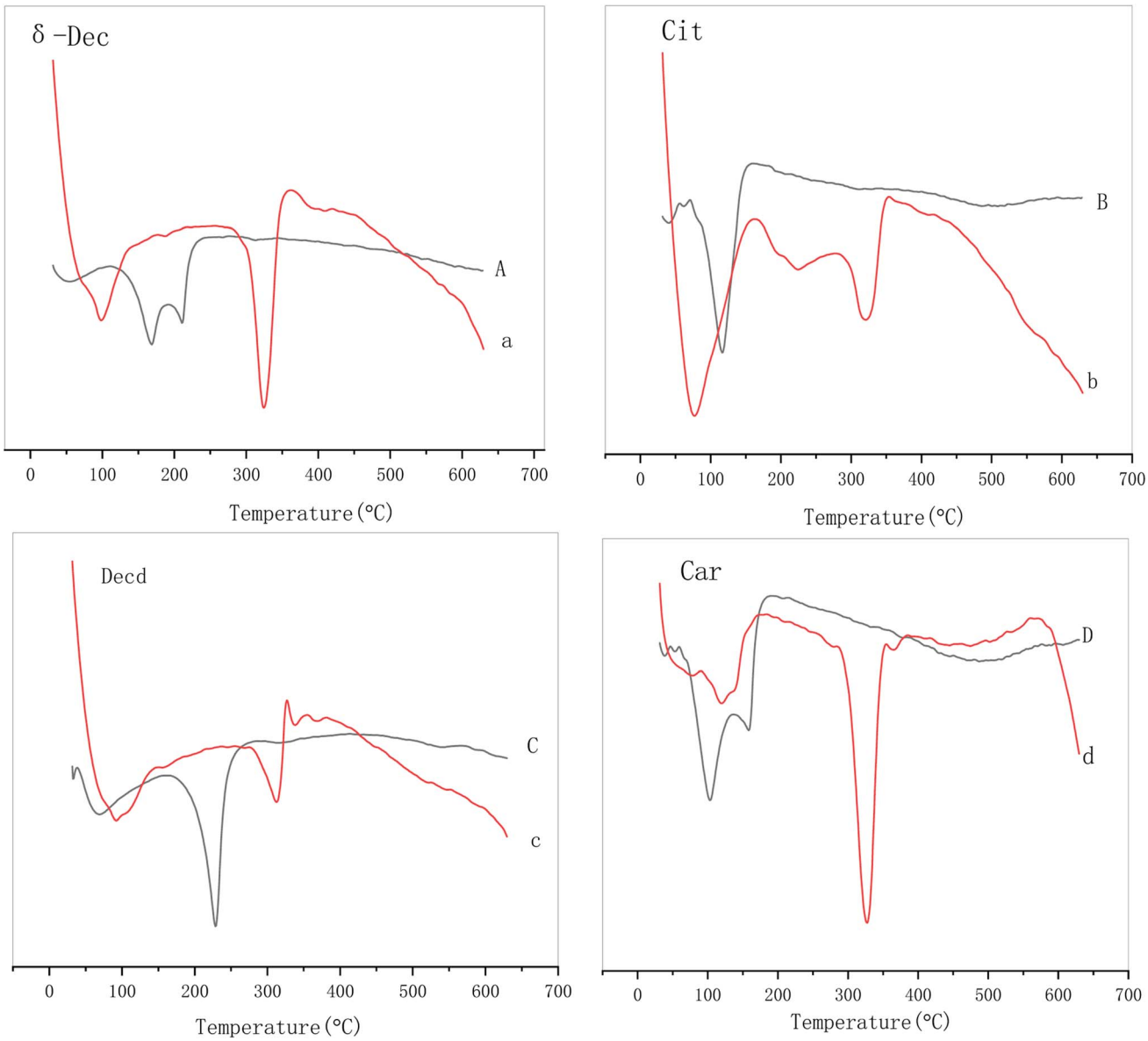

Fig. 6 DSC of different aromatic molecules complexed with LRCD (abcd: aromatic compounds, ABCD matching to the complex) where A is δ-decanolactone inclusion, B is citral inclusion, C is decanoic acid inclusion, D is carvone inclusion.

around 100 °C may be associated with water evaporation because of the dissolution of hydrogen bonds that hold water in the sample's crystalline zone. Second, there is a notable exothermic peak at temperatures above 250 °C, indicating the breakdown of the inclusion complex created by the guest molecule and LRCD complexing. Citral exhibits a single endothermic peak on the DSC curve, whereas other guest substances exhibit two phases (endothermic and decomposition phases). The evaporation of water molecules is responsible for one endothermic peak at approximately 100 °C, while the decomposition of its own structure results in an exothermic peak at temperatures between 150 and 250 °C. When the DSC curves of the claths and the guest molecules are compared, it can be shown that the claths' decomposition temperature, which ranges from 300 to 350 °C, is greater than that of the free guest molecules. This can suggest that the claths' structure is more stable, possibly because the guest molecules and LRCD form the clathrates. However, the decomposition temperature of the exothermic peaks varies due to the different structures of the guest molecules. This finding is consistent with the results reported by Gao *et al.*,[24] and the above analysis results are also in agreement with those from TGA, indicating that the thermal stability of aromatic molecules is enhanced when they form inclusion complexes with LRCD.

4. Conclusions

LRCD was able to successfully encapsulate aroma compounds. XRD, FTIR, NMR and TGA techniques were used to examine the effects of different aromatic chemical compounds on the LRCD

clones and the changes in the cavity structure of LRCD. Different aroma compounds exhibit consistent variations in spatial conformation, crystallinity, and thermal stability, and LRCD can embed tiny molecules to create compact clathrates. The LRCD prefers to form a folded coil around the guest molecule and has significantly less conformational mobility when it is present. The creation of compact structures in the inclusion complexes is facilitated by the greater contacts that aromatic chemical molecules with long alkyl and cycloalkyl chains, strong hydrophobic functional groups, and smaller cross-sections have with CD cavities. The final guest molecule was encapsulated in the CD cavity with low embedding after complexes containing lactones or aromatic groups were folded during the simulation. This was in accordance with the experiment's findings, which showed that carvone had the highest embedding efficiency and δ-decanolactone the lowest aroma compounds/LRCD inclusion complexes can increase the thermal stability of aroma compounds, and inclusion complexes are formed according to all analytical techniques. Thus, complexation with LRCD can be an efficient way to enhance the use of aroma compounds in the food and pharmaceutical industries, and this study advances knowledge of the interaction between LRCD and aroma compounds, which may be utilised as a possible solid matrix carrier for the encapsulation of aroma/flavor compounds in the food industry.

The study has a number of limitations in spite of these revelations. In order to limit the generalizability of the findings to aromatic compounds with longer carbon chains or more complex functional group combinations (such as polycyclic aromatics or compounds with heteroatoms), the study first concentrated on four C10 aromatic compounds with particular functional groups (aldehyde, ketone, lactone, and carboxylic acid). The behavior of LRCD-aromatic complexes in dynamic systems (such as simulated gastrointestinal environments or food processing conditions with variable temperature, pH, and mechanical stress) has not been defined because the experiments were carried out *in vitro* under static conditions.

Future research should concentrate on the following areas in order to overcome these constraints and increase the useful uses of LRCD-aromatic complexes: increasing the range of visitor molecules: to create a more thorough foundation for the structure–activity relationship, LRCD complexation with aromatic compounds of different carbon chain lengths and functional groups (such as ethers, esters, or halogenated aromatics) is being investigated. Assessing intricate dynamics in dynamic systems: to confirm that LRCD-aromatic compounds are suitable for industrial and biomedical applications, their stability, release kinetics, and bioavailability are evaluated under physiological and food processing simulations, such as high-temperature sterilization and gastric digestion. Enhancing intricate preparation: creating scalable manufacturing techniques for the large-scale synthesis of LRCD-aromatic complexes and investigating modified LRCD derivatives (such as alkylated or hydroxylated LRCD) to improve guest specificity and encapsulation efficiency. Future studies can improve the theoretical underpinnings of LRCD-based encapsulation and hasten its adoption in industrial settings by tackling these issues.

Author contributions

Chuan Cao: data curation, software, validation. Pingping Huang: methodology, investigation, formal analysis. Jing Guo: resources, project administration, funding acquisition. Deming Li: writing – review & editing, supervision, conceptualization.

Conflicts of interest

The authors declare no conflicts of interest.

Data availability

The data generated and analyzed during this study are available from the corresponding author upon reasonable request. The NMR data and other experimental data supporting the findings of this study have been included in the revised manuscript. The raw data of LRCD preparation, inclusion complex characterization, and related statistical analyses are properly stored and can be provided for verification purposes if needed.

Acknowledgements

This study received support from the Caochuan Project, an excellent young teacher cultivation project in 2024, with project number YQZD2024082. This work was also supported by the Youth Top-Notch Talent (Young Famous Teacher) Program of the 2025 Anhui High-End Talent Recruitment and Training Action, awarded to Cao Chuan.

References

1 I. Benalaya, G. Alves, J. Lopes and L. R. Silva, *Int. J. Mol. Sci.*, 2024, **25**(2), 1322–1335.
2 S. Machida, S. Ogawa, S. Xiaohua, T. Takaha, K. Fujii and K. Hayashi, *FEBS Lett.*, 2020, **486**(2), 131–136.
3 K. Teranishi, T. Nishiguchi and H. Ueda, *Carbohydr. Res.*, 2003, **338**, 987–993.
4 Y. Terada, M. Yanase and H. Takata, *J. Biol. Chem.*, 1997, **272**(25), 15729–15733.
5 M. T. etTadashi Gomi, *Chem. Pharm. Bull.*, 2002, **44**, 2086–2091.
6 T. Furuishi, Y. Ohmachi, T. Fukami, H. Nagase, T. Suzuki, T. Endo, H. Ueda and K. Tomono, *J. Incl. Phenom. Macrocycl. Chem.*, 2010, **67**, 233–239.
7 T. M. Almeleebia, N. Goyal, M. H. Akhter, A. Alalmaie, A. I. Al-Harbi, H. Khalilullah, M. S. Ali, M. I. Alam, S. Ahmad and N. Alam, *J. Clust. Sci.*, 2025, **36**(1), 13.
8 H. Takata, T. Takaha, H. Nakamura, K. Fujii, S. Okada, M. Takagi, T. Imanaka and J. Ferment, *Bioeng.*, 1997, **84**, 119–123.
9 J. Szejtli, *Pergamon*, 1996, **3**, 423–440.
10 C. Cao, L. Xu, P. Xie, J. Hu, J. Qi, Y. Zhou and L. Cao, *RSC Adv.*, 2020, **10**, 6584–6591.

11 C. Cao, P. Xie, Y. Zhou and J. Guo, *Foods*, 2023, **12**, 15.
12 M. D. C. Antunes and A. M. Cavaco, *Flavour Fragr. J.*, 2010, **25**, 351–366.
13 J. L. Koontz, J. E. Marcy, S. F. O'keefe and S. E. Duncan, *J. Agric. Food Chem.*, 2009, **57**, 1162–1171.
14 P. J. Fei, Q. C. Xiao, Z. Y. Hong and Y. Ling, *J. Food Process. Preserv.*, 2010, **34**, 114–124.
15 R. Ficarra, S. Tommasini and D. Raneri, *J. Pharm. Biomed. Anal.*, 2002, **29**(6), 1005–1014.
16 Y. Nait Bachir, R. Nait Bachir and A. Hadj-Ziane-Zafour, *Drug Dev. Ind. Pharm.*, 2019, **45**, 333–347.
17 M. Shrestha, T. M. Ho and B. R. Bhandari, *Food Chem.*, 2017, **221**, 1474–1483.
18 Q. Nguyen and P. T. Southwell-Keely, *Lipids*, 2007, **42**, 171–178.
19 C. Cao, D. Wei, L. Xu, J. Hu, J. Qi and Y. Zhou, *J. Sci. Food Agric.*, 2021, **101**, 2877–2883.
20 A. R. Hedges, J. S. Wen and C. T. Sikorski, *Use of Cyclodextrins for Encapsulation in the Use and Treatment of Food Products*, 1995.
21 L. E. Hill, C. Gomes and T. M. Taylor, *LWT - Food Sci. Technol.*, 2013, **51**, 86–93.
22 L. M. M. Gomes, N. Petito, V. G. Costa, D. Q. Falcão and K. G. D. L. Araújo, *Food Chem.*, 2014, **148C**, 428–436.
23 T. A. Misharina, M. B. Terenina and N. I. Krikunova, *Appl. Biochem. Microbiol.*, 2002, **38**(6), 583–587.
24 Q. Gao, B. Zhang, L. Qiu, X. Fu and Q. Huang, *Food Hydrocoll.*, 2020, **108**, 105969.
25 U. V. L. Ma, J. D. Floros and G. R. Ziegler, *Carbohydr. Polym.*, 2011, **83**, 1869–1878.
26 V. E. de Oliveira, E. W. C. Almeida, H. V Castro, H. G. M. Edwards, H. F. Dos Santos and L. F. C. de Oliveira, *J. Phys. Chem. A*, 2011, **115**, 8511–8519.
27 J. G. Galvão, V. F. Silva, S. G. Ferreira, F. R. M. França, D. A. Santos, L. S. Freitas, P. B. Alves, A. A. S. Araújo, S. C. H. Cavalcanti and R. S. Nunes, *Thermochim. Acta*, 2015, **608**, 14–19.
28 K. Kuttiyawong, S. Saehu, K. Ito and P. Pongsawasdi, *Process Biochem.*, 2015, **50**, 2168–2176.
29 L. Lin, Y. Zhu and H. Cui, *Lwt*, 2018, **97**, 711–718.
30 J. A. Putseys, L. J. Derde, L. Lamberts, H. Goesaert and J. A. Delcour, *Carbohydr. Polym.*, 2009, **78**, 854–861.
31 O. Nimz, K. Gessler, I. Usón, G. M. Sheldrick and W. Saenger, *Carbohydr. Res.*, 2004, **339**, 1427–1437.
32 L. Yeo, D. B. Thompson and D. G. Peterson, *Food Chem.*, 2016, **199**, 393–400.
33 G. Delogu, C. C. A. Juliano and M. Usai, *Nat. Prod. Res.*, 2016, **30**, 2049–2057.
34 G. G. Gelders, J. P. Duyck, H. Goesaert and J. A. Delcour, *Carbohydr. Polym.*, 2005, **60**, 379–389.
35 C. Heinemann, B. Conde-Petit, J. Nuessli and F. Escher, *J. Agric. Food Chem.*, 2001, **49**, 1370–1376.
36 D. H. Kringel, M. D. Antunes, B. Klein, R. L. Crizel, R. Wagner, R. P. de Oliveira, A. R. G. Dias and E. da R. Zavareze, *J. Food Sci.*, 2017, **82**, 2598–2605.
37 X. Cai, X. Du, D. Cui, X. Wang, Z. Yang and G. Zhu, *Food Hydrocoll.*, 2019, **91**, 238–245.